# Supplement to: FRIDA-Clim v1.0.0: a Simple Climate Model with Process-Based Carbon Cycle used in the FRIDAv2.1 IAM

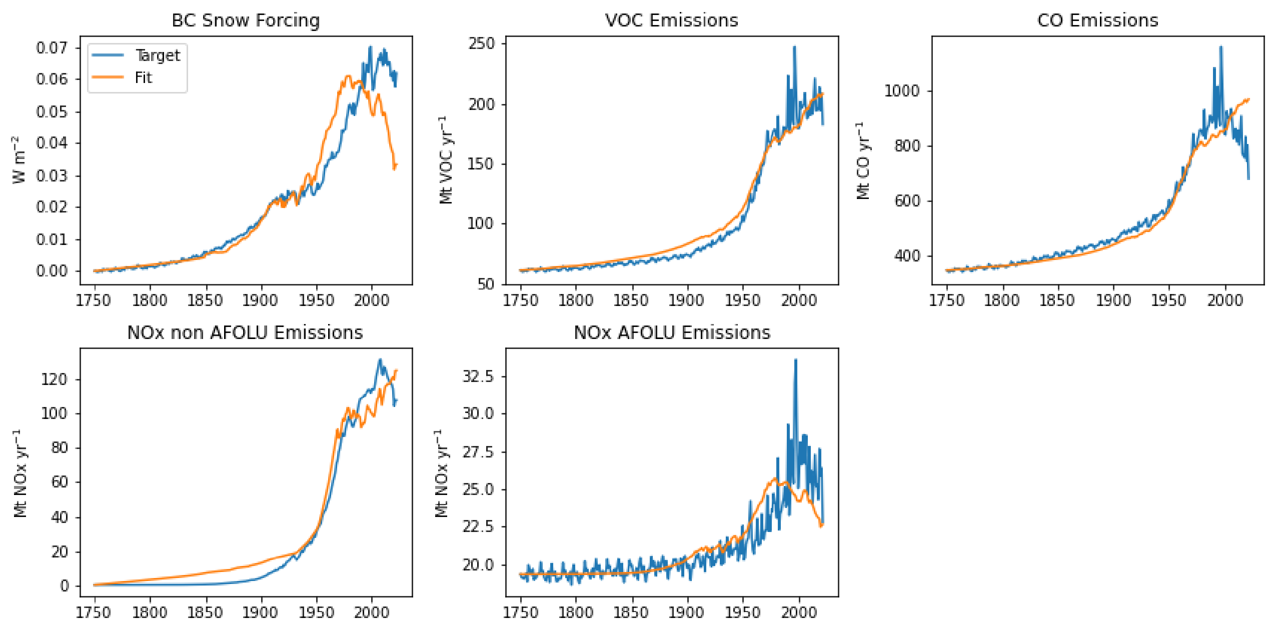


**Figure S1: Regression predictions of $NO_x$, VOC, and CO emissions, and the BC Snow forcing; see Section 2.1 for details.**

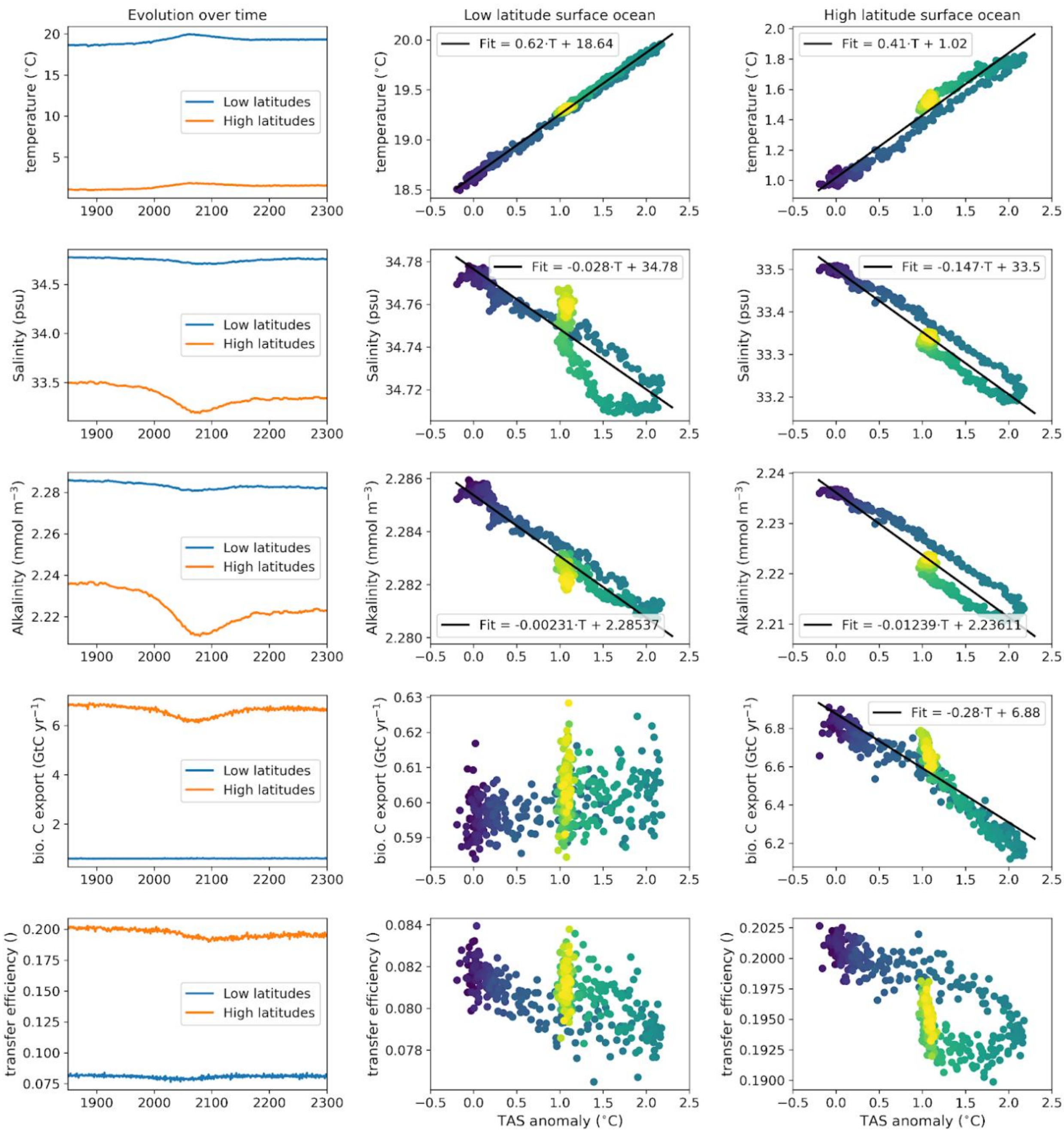


**Figure S2: Analysis of MPI-ESM1.2-LR emission-driven simulations of the SSP5-3.4-over scenario used to inform the ocean carbon module in FRIDA. Each row represent a different quantity (from top to bottom): surface ocean temperature, surface ocean salinity, surface ocean alkalinity (all averaged over the upper 90 m of the ocean), downward export of biological carbon out of the surface layer and fraction of carbon that is exported below 1000 m depth (transfer efficiency). The left column shows the evolution**

**of the MPI-ESM1.2-LR data as time series, and the middle and right columns show their relationship to the global mean temperature anomaly for the low and high latitude surface ocean respectively. A regression line is plotted for those quantities that are parameterized via a linear temperature relationship in FRIDA-Clim. Data taken from https://esgf-metagrid.cloud.dkrz.de/search; for more information see https://cmiphub.cloud.dkrz.de/esgf-projects/mpi-edriven-le.php and** Li et al., (2023).

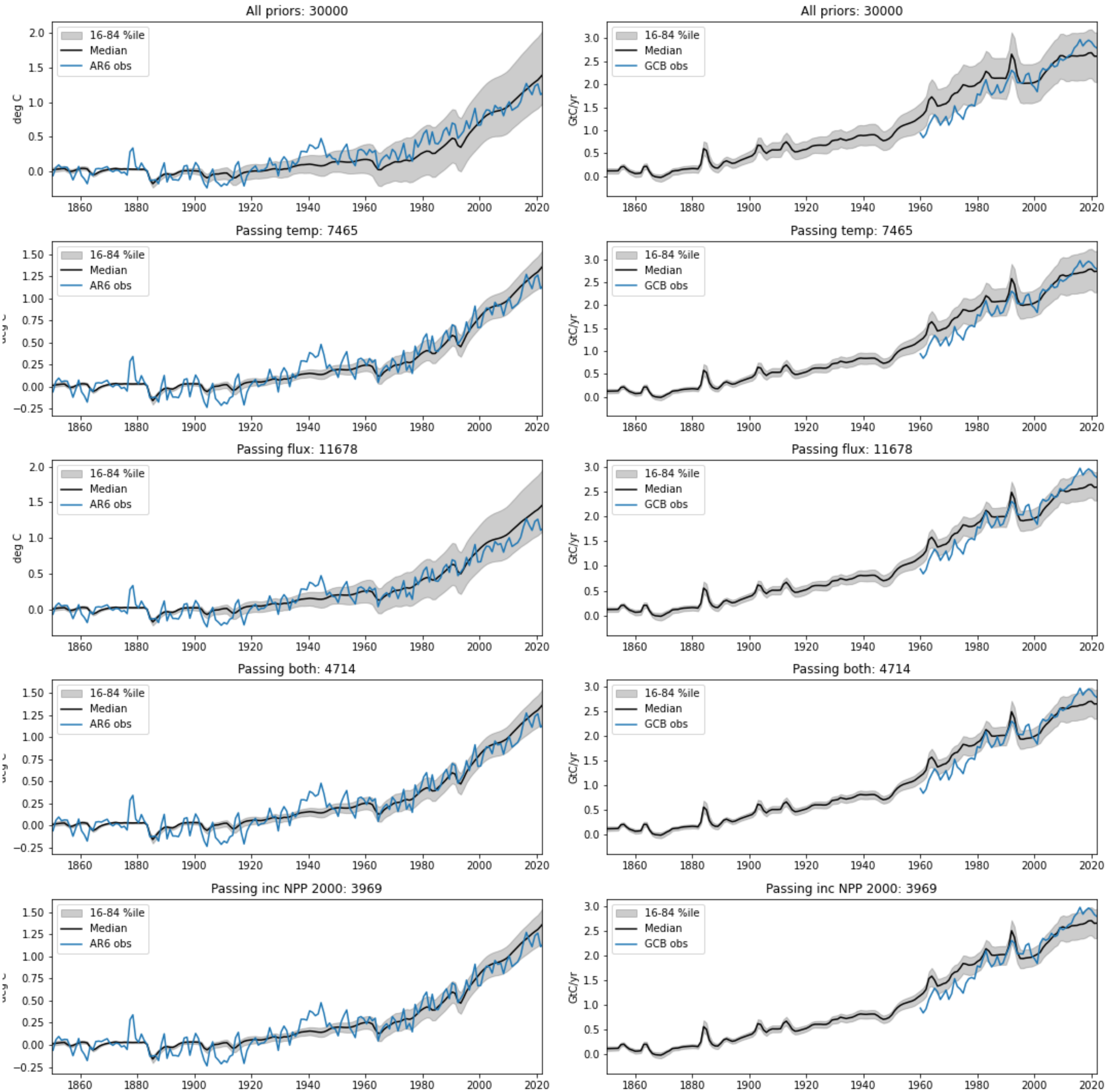


**Figure S3: The initial constraints applied to the 30,000 member priors in FRIDA-Clim, and their effects on the ensemble GMST (left) and air-sea $CO_2$ flux (right). The prior ensemble (top row) is reduced to 7,000-11,000 members when the GMST and air-sea $CO_2$ flux constraints are applied separately (2nd and 3rd rows), and just over 4,500 when applied together (4th row). The single-year NPP constraint further reduces this to 3,969 members, completing the initial constraints step (bottom row).**

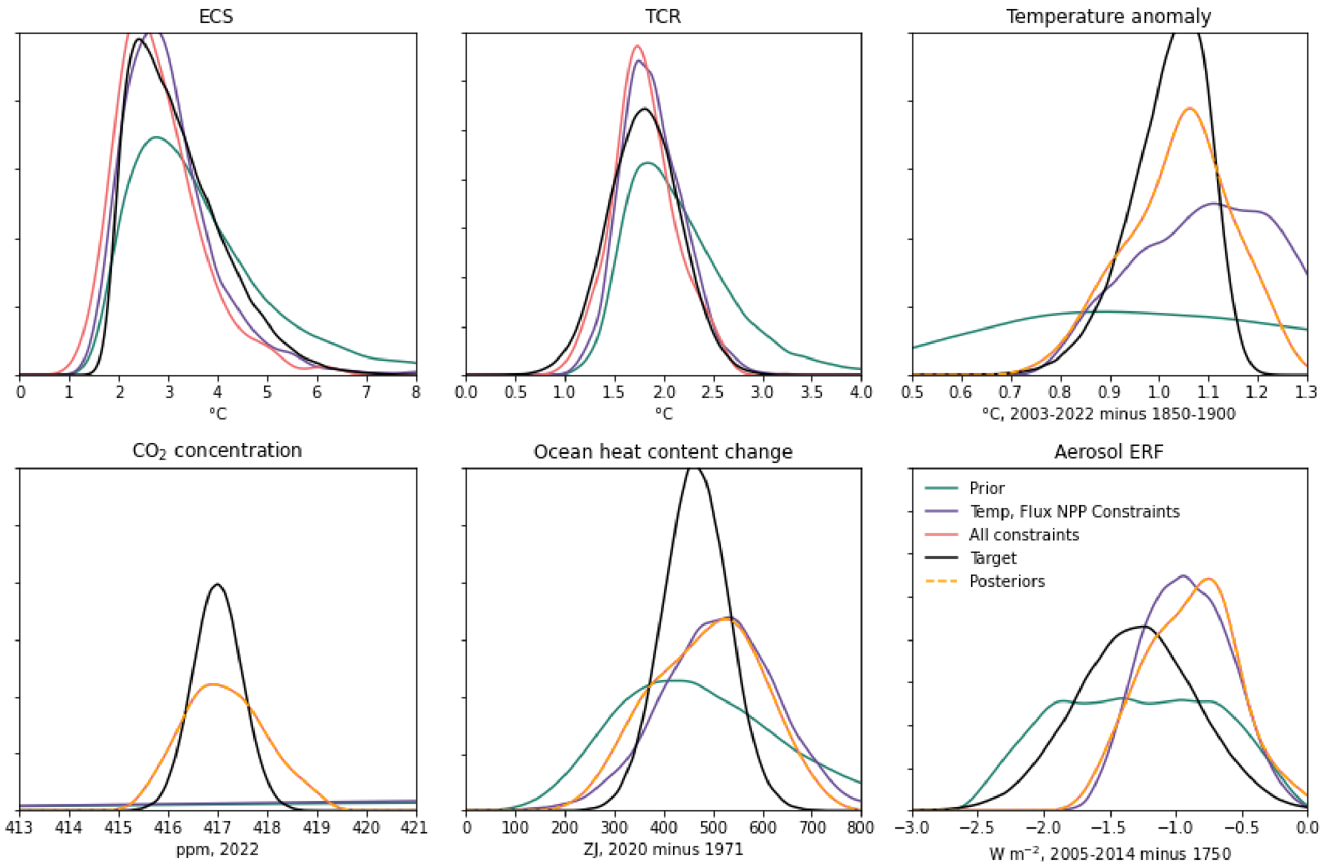


**Figure S4: The application of the distributional constraints to the FRIDA-Clim ensemble. Shown are the distributions of the variables used in the constraining process (Figure 4), for the target reference distributions, the 30,000 priors, the 3,969 members passing the initial constraints, the 100 members selected in this distributional constraining step, and the results of running these 100 members through FRIDA-Clim again to verify their consistency.**

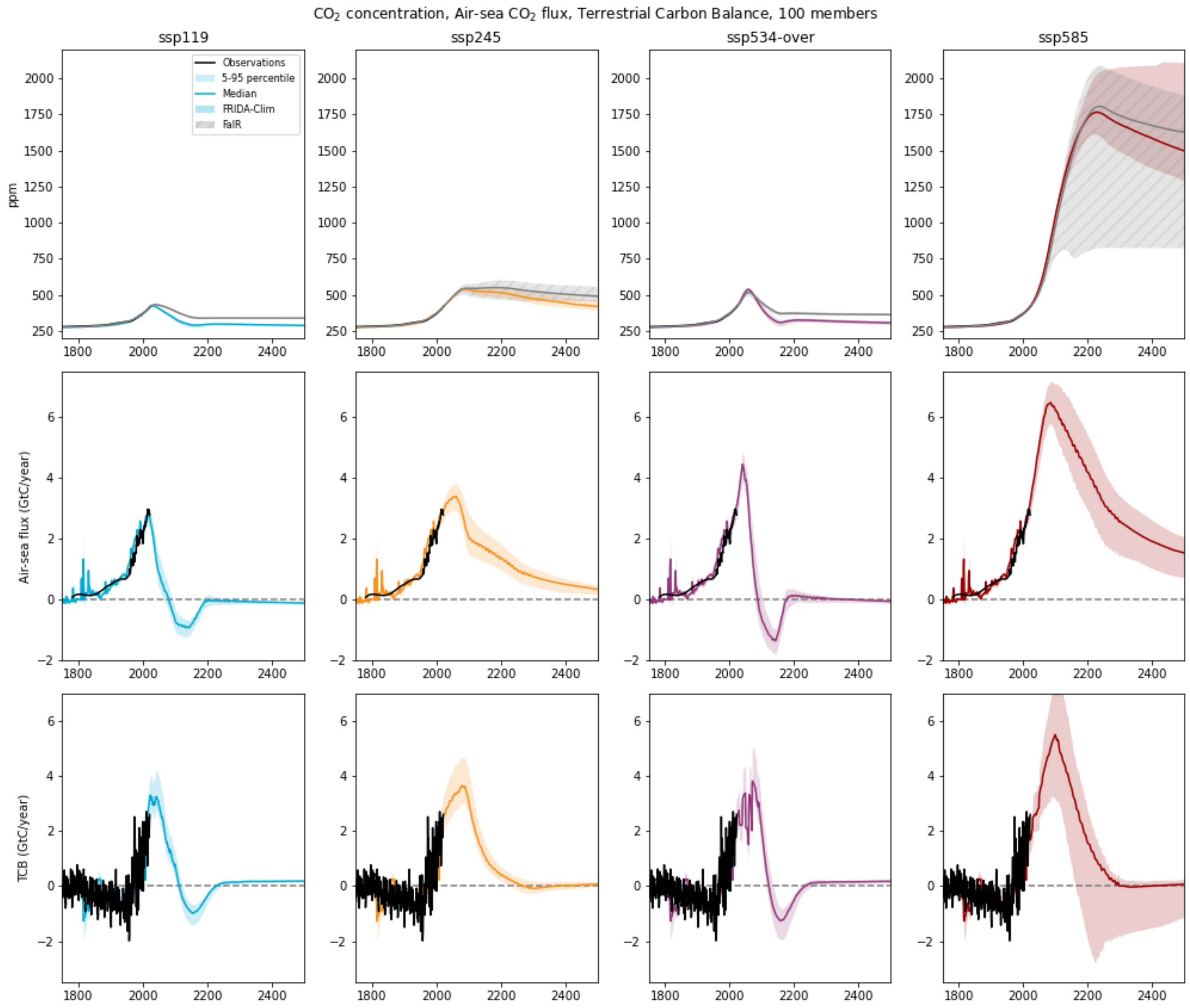


**Figure S5: As for the top row of Figure 6, instead showing $CO_2$ concentration (top), air-sea $CO_2$ flux (middle), and terrestrial carbon balance (bottom), along with observations for each (**Smith et al., (2024) **for $CO_2$, and** Friedlingstein et al., (2025) **for the carbon fluxes). Note that this data is produced with a version of FRIDA-Clim calibrated to RCMIP emissions (see main text).**

| **Variable Name** | **Units** | **Treatment within climate calibration** |
|---|---|---|
| Energy Balance Model Parameters | | |

| | | |
|---|---|---|
| Energy Balance Model.Heat Capacity of Land & Ocean Surface | W $yr^{-1}$ $metre^{-2}$ $K^{-1}$ | Sampled based on $4xCO_2$ Earth System Model data as in Smith, Cummins, et al., (2024). |
| Energy Balance Model.Heat Capacity of Thermocline Ocean | W $yr^{-1}$ $metre^{-2}$ $K^{-1}$ | " |
| Energy Balance Model.Heat Capacity of Deep Ocean | W $yr^{-1}$ $metre^{-2}$ $K^{-1}$ | " |
| Energy Balance Model.Deep Ocean Heat Uptake Efficacy Factor | Dimensionless | " |
| Energy Balance Model.Heat Transfer Coefficient between Land & Ocean Surface and Space | W $metre^{-2}$ $K^{-1}$ | " |
| Energy Balance Model.Heat Transfer Coefficient between Surface and Thermocline Ocean | W $metre^{-2}$ $K^{-1}$ | " |
| Energy Balance Model.Heat Transfer Coefficient between Thermocline Ocean and Deep Ocean | W $metre^{-2}$ $K^{-1}$ | " |
| Radiative Forcing Parameters | | |
| $CO_2$ Forcing.Atmospheric $CO_2$ Concentration 1750 * | ppm | Sampled as in Smith, Cummins, et al., (2024). |
| Aerosol Forcing.Scaling Aerosol Cloud Interactions Effective Radiative Forcing scaling factor | W $metre^{-2}$ | " |
| Aerosol Forcing.Logarithmic Aerosol Cloud Interactions Effective Radiative Forcing scaling | $1/(MtSO_2\ yr^{-1})$ | " |

| | | |
|---|---|---|
| factor | | |
| Aerosol Forcing.Effective Radiative Forcing from Aerosol Radiation Interactions per unit $SO_2$ Emissions | (W metre$^{-2}$))/(Mt$SO_2$ yr$^{-1}$) | “ |
| $CH_4$ Forcing.Calibration scaling of $CH_4$ forcing | Dimensionless | “ |
| $N_2O$ Forcing.Calibration scaling of $N_2O$ forcing | Dimensionless | “ |
| Minor GHGs Forcing.Calibration scaling of Minor GHG forcing | Dimensionless | “ |
| Stratospheric Water Vapour Forcing.Calibration scaling of Stratospheric H2O forcing | Dimensionless | “ |
| BC on Snow Forcing.Calibration scaling of Black Carbon on Snow forcing | Dimensionless | “ |
| Land Use Forcing.Calibration scaling of Albedo forcing | Dimensionless | “ |
| Land Use Forcing.Calibration scaling of Irrigation forcing | Dimensionless | Sampled as a skewnorm distribution to match Forster et al., (2021) estimates of -0.05 (-0.10 to 0.05) W/m2 in the present-day. |
| Natural Forcing.Calibration scaling of Volcano forcing | Dimensionless | Sampled as in Smith, Cummins, et al., (2024). |
| $CO_2$ Forcing.Calibration scaling of $CO_2$ forcing | Dimensionless | “ |
| Natural Forcing.Amplitude of Effective Radiative Forcing from Solar Output Variations | Dimensionless | “ |
| Natural Forcing.Linear trend in Effective Radiative Forcing from Solar Output Variations | W metre$^{-2}$ yr$^{-1}$ | “ |

| | | |
|---|---|---|
| Ozone Forcing.Ozone forcing per unit $CH_4$ concentration change | W metre$^{-2}$ ppb$^{-1}$ | “ |
| Ozone Forcing.Ozone forcing per unit $N_2O$ concentration change | W metre$^{-2}$ ppb$^{-1}$ | “ |
| Ozone Forcing.Ozone forcing per unit Montreal gases equivalent effective stratospheric chlorine concentration change | W metre$^{-2}$ CFC11eq$^{-1}$ | “ |
| Ozone Forcing.Ozone forcing per unit CO emissions change | (W metre$^{-2}$)/(Mt CO yr$^{-1}$) | “ |
| Ozone Forcing.Ozone forcing per unit VOC emissions change | (W metre$^{-2}$)/(MtVOC yr$^{-1}$) | “ |
| Ozone Forcing.Ozone forcing per unit $NO_x$ emissions change | (W metre$^{-2}$)/(Mt$NO_x$ yr$^{-1}$) | “ |
| Ocean Parameters | | |
| Ocean.Depth of warm surface ocean layer * | Metres | Uniformly sampled in the ocean spinup between 50 and 500. |
| Ocean.Thickness of intermediate ocean layer * | Metres | Uniformly sampled in the ocean spinup between 300 and 1000. |
| Ocean.Depth of cold surface ocean layer * | Metres | Uniformly sampled in the ocean spinup between 50 500. |
| Ocean.Reference overturning strength in Sv * | Sverdrup | Uniformly sampled in the ocean spinup between 10 and 30. |
| Ocean.Reference intermediate to warm surface ocean mixing strength * | Sverdrup | Uniformly sampled in the ocean spinup between 50 and 90. |
| Ocean.Reference cold surface to deep ocean | Sverdrup | Uniformly sampled in the ocean spinup |

| | | |
|---|---|---|
| mixing strength * | | between 10 and 30. |
| Ocean.Reference strength of biological carbon pump in low latitude ocean * | GtC $yr^{-1}$ | Uniformly sampled in the ocean spinup between 0 and 3. |
| Ocean.Reference strength of biological carbon pump in high latitude ocean * | GtC $yr^{-1}$ | Uniformly sampled in the ocean spinup between 4 and 12. |
| Ocean.High latitude carbon pump transfer efficiency * | Dimensionless | Uniformly sampled in the ocean spinup between 0.1 and 0.5. |
| Ocean.Warm surface ocean alkalinity sensitivity to global T anomaly | $K^{-1}$ | Uniformly sampled in the historical prior ensemble between -4E-6 and -1E-6. |
| Ocean.Cold surface ocean alkalinity sensitivity to global T anomaly | $K^{-1}$ | Uniformly sampled in the historical prior ensemble between -3E-5 and -5E-6. |
| Ocean.High latitude carbon pump sensitivity to global T anomaly | GtC $yr^{-1}$ $K^{-1}$ | Uniformly sampled in the historical prior ensemble between -0.5 and 0. |
| Ocean.Warm surface ocean temperature sensitivity to global T anomaly | Dimensionless | Uniformly sampled in the historical prior ensemble between 0.4 and 1.0. |
| Ocean.Cold surface ocean temperature sensitivity to global T anomaly | Dimensionless | Uniformly sampled in the historical prior ensemble between 0.3 and 1.0. |
| Ocean.Warm surface ocean salinity sensitivity to global T anomaly | $K^{-1}$ | Uniformly sampled in the historical prior ensemble between -0.04 and -0.01- co-varying with the warm surface alkalinity sensitivity. |
| Ocean.Cold surface ocean salinity sensitivity to global T anomaly | $K^{-1}$ | Uniformly sampled in the historical prior ensemble between -0.3 and -0.05 - co-varying with the warm surface |

| | | |
|---|---|---|
| | | alkalinity sensitivity. |
| Land model parameters (FRIDA-Clim only) | | |
| Crop.normal harvest index for food crops** | Dimensionless | Uniformly sampled in the spinup between 0.4 and 0.45. |
| Crop.sensitivity of effect of crop yield on harvest index** | Dimensionless | Uniformly sampled in the spinup between 0.05 and 0.1. |
| Crop.crop yield 1980 reference** | PCal $Mha^{-1}$ $yr^{-1}$ | Uniformly sampled in the spinup between 5.5 and 6.5. |
| Crop.harvest index for feed crops** | Dimensionless | Uniformly sampled in the spinup between 0.5 and 0.8. |
| Crop.sensitivity of effect of crop residue production on field fraction** | Dimensionless | Uniformly sampled in the spinup between 0 and 0.75. |
| soil carbon decay.cropland litter input share slow soil carbon** | Dimensionless | Uniformly sampled in the spinup between 0.01 and 0.03. |
| soil carbon decay.grassland litter input share slow soil carbon** | Dimensionless | Uniformly sampled in the spinup between 0.01 and 0.03. |
| soil carbon decay.mature forest litter input share slow soil carbon** | Dimensionless | Uniformly sampled in the spinup between 0.015 and 0.035. |
| soil carbon decay.young forest litter input share slow soil carbon** | Dimensionless | Uniformly sampled in the spinup between 0.01 and 0.035. |
| soil carbon decay.natural decay rate fast soil carbon** | $yr^{-1}$ | Uniformly sampled in the spinup between 0.025 and 0.035. |
| soil carbon decay.natural decay rate litter carbon** | $yr^{-1}$ | Uniformly sampled in the spinup between 0.6 and 0.8. |

| | | |
|---|---|---|
| soil carbon decay.natural decay rate slow soil carbon** | $yr^{-1}$ | Uniformly sampled in the spinup between 0.0008 and 0.0012. |
| soil carbon decay.e0** | K | Uniformly sampled in the spinup between 290 and 300. |
| soil carbon decay.temp_response** | K | Uniformly sampled in the spinup between 55 and 60. |
| degraded land soil carbon.degraded land productivity reduction factor** | Dimensionless | Uniformly sampled in the spinup between 0.01 and 0.1. |
| Land Use.forest recovery time** | yr | Uniformly sampled in the spinup between 50 and 70. |
| Forest.tree net primary production in 1750** | GtC $Mha^{-1}$ $yr^{-1}$ | Uniformly sampled in the spinup between 0.005 and 0.0095. |
| Grass.grass net primary production in 1750** | GtC $Mha^{-1}$ $yr^{-1}$ | Uniformly sampled in the spinup between 0.0035 and 0.005. |
| Forest.forest aboveground biomass 1750** | GtC | Uniformly sampled in the spinup between 500 and 700. |
| Land Use.Initial young forest area**,[a] | Mha | Uniformly sampled in the spinup between 50 and 300. |
| Forest.Young mature forest biomass ratio**,[a] | Dimensionless | Uniformly sampled in the spinup between 0.3 and 0.7. |
| Forest.$CO_2$ tree net primary production parameter | $ppm^{-1}$ | Uniformly sampled in the historical prior ensemble between 0.0008 and 0.0012. |
| Forest.STA maximum aboveground biomass per area parameter | $K^{-1}$ | Uniformly sampled in the historical prior ensemble between 0.3 and 0.5. |

| | | |
|---|---|---|
| Forest.STA squared maximum aboveground biomass per area parameter | $K^{-2}$ | Uniformly sampled in the historical prior ensemble between -0.05 and -0.02. |
| Forest.STA squared tree net primary production parameter | $K^{-2}$ | Uniformly sampled in the historical prior ensemble between -0.05 and -0.01. |
| Forest.STA tree net primary production parameter | $K^{-1}$ | Uniformly sampled in the historical prior ensemble between 0.1 and 0.15. |
| Grass.$CO_2$ grass net primary production parameter | $ppm^{-1}$ | Uniformly sampled in the historical prior ensemble between 0.0008 and 0.0012. |
| Grass.STA grass net primary production parameter | $K^{-1}$ | Uniformly sampled in the historical prior ensemble between 0.1 and 0.15. |
| Grass.STA squared grass net primary production parameter | $K^{-2}$ | Uniformly sampled in the historical prior ensemble between -0.05 and -0.1. |
| Crop.harvest index for energy crops | Dimensionless | Uniformly sampled in the historical prior ensemble between 0.6 and 0.95. |

**Table S1: the parameters varied within the model calibration, along with their units and some summary information on their treatment within the procedure. Also listed are the output stocks from the Climate Module calibration to FRIDAv2.1. *The 10 parameters varied in the ocean spinup in the Climate Module. **The 21 land parameters additionally varied in the FRIDA-Clim spinup. [a]These two forest parameters are varied in the FRIDA-Clim spinup, but redundant in the priors due to the use of the young and mature forest area and biomass stocks. See the Code Availability section for the calibration procedure code.**

| Parameter name in main text | Units | Value in FRIDA-Clim v1.0.0 |
|---|---|---|
| $f_1^{CO_2}$ | W $m^{-2}$ | 4.57 |
| $f_3^{CO_2}$ | W $m^{-2}$ $ppm^{-1/2}$ | 0.086 |
| $f_3^{CH_4}$ | W $m^{-2}$ $ppb^{-1/2}$ | 0.038 |
| $f_3^{N_2O}$ | W $m^{-2}$ $ppb^{-1/2}$ | 0.106 |
| $A_{oceans}$ | m | $3.6\times10^{14}$ |
| $F^i$ | dimensionless | 0.85 / 0.15 for warm / cool ocean |

| | |
|---|---|
| $f_1^{ACI}$ | Aerosol Forcing.Scaling Aerosol Cloud Interactions Effective Radiative Forcing scaling factor |
| $f_1^{ARI}$ | Aerosol Forcing.Logarithmic Aerosol Cloud Interactions Effective Radiative Forcing scaling factor |
| $F_{SO_2}$ | Aerosol Forcing.Effective Radiative Forcing from Aerosol Radiation Interactions per unit $SO_2$ Emissions |
| a | Forest.STA tree net primary production parameter;<br>Grass.STA grass net primary production parameter |
| b | Forest.STA squared tree net primary production parameter;<br>Grass.STA squared grass net primary production parameter |
| c | Forest.$CO_2$ tree net primary production parameter;<br>Grass.$CO_2$ grass net primary production parameter |
| d | Forest.STA maximum aboveground biomass per area parameter |
| e | Forest.STA squared maximum aboveground biomass per area parameter |
| $e_0$ | soil carbon decay.e0 |
| $R$ | soil carbon decay.temp_response |

**Table S2: units and values of parameters referred to in the main text. Non-constant parameters are referred to their model names in Table S1.**

| Full Model Calibration Variable | Calibration Data Source |
|---|---|
| $CO_2$ Emissions | See Table 1 |
| $CO_2$ Emissions from Energy | “ |
| $CO_2$ Emissions from Food and Land Use | “ |
| $N_2O$ Emissions from Food and Land Use | “ |
| $N_2O$ Emissions from Other | “ |
| $N_2O$ Emissions from Energy | “ |
| $CH_4$ Emissions from Energy | “ |

| | |
|---|---|
| $CH_4$ Emissions from Food and Land Use | “ |
| $CH_4$ Emissions from Other | “ |
| $SO_2$ Emissions from Energy | “ |
| $SO_2$ Emissions from Food and Land Use | “ |
| HFC134a-eq Emissions | “ |
| CO Emissions | CEDS v2024_07_08 plus GFED BB4CMIP. (Hoesly et al., 2024; van Marle et al., 2017) |
| VOC Emissions | “ |
| $NO_x$ non AFOLU Emissions | CEDS sectors 1, 2, 5, 6, and 7. |
| $NO_x$ AFOLU Emissions | CEDS sector 3, plus GFED. |
| Total $CH_4$ Emissions | Summed over sectors. |
| Total $CO_2$ Emissions | “ |
| Total $SO_2$ Emissions | “ |
| Total $N_2O$ Emissions | “ |
| Total $NO_x$ Emissions | “ |
| $CO_2$ Effective Radiative Forcing | Indicators of Global Climate Change (Smith, Walsh, et al., 2024) |
| $CH_4$ Effective Radiative Forcing | “ |
| $N_2O$ Effective Radiative Forcing | “ |
| Atmospheric $CO_2$ Concentration | “ |
| Atmospheric $N_2O$ Concentration | “ |
| Atmospheric $CH_4$ Concentration | “ |

| | |
|---|---|
| Energy Balance Model.Surface Temperature Anomaly | “ |

**Table S3: the variables associated with the Climate Module which are included within the full model calibration, and their data sources. See Code Availability for code containing full details and procedure.**

**References**

Forster, P., Storelvmo, T., Armour, K., Collins, W., Dufresne, J.-L., Frame, D., Lunt, D. J., Mauritsen, T., Palmer, M. D., Watanabe, M., Wild, M., & Zhang, H. (2021). The Earth’s Energy Budget, Climate Feedbacks, and Climate Sensitivity. In V. Masson-Delmotte, P. Zhai, A. Pirani, S. L. Connors, C. Péan, S. Berger, N. Caud, Y. Chen, L. Goldfarb, M. I. Gomis, M. Huang, K. Leitzell, E. Lonnoy, J. B. R. Matthews, T. K. Maycock, T. Waterfield, O. Yelekçi, R. Yu, & B. Zhou (Eds.), *Climate Change 2021: The Physical Science Basis. Contribution of Working Group I to the Sixth Assessment Report of the Intergovernmental Panel on Climate Change* (pp. 923–1054). Cambridge University Press. https://doi.org/10.1017/9781009157896.009

Friedlingstein, P., O’Sullivan, M., Jones, M. W., Andrew, R. M., Hauck, J., Landschützer, P., Le Quéré, C., Li, H., Luijkx, I. T., Olsen, A., Peters, G. P., Peters, W., Pongratz, J., Schwingshackl, C., Sitch, S., Canadell, J. G., Ciais, P., Jackson, R. B., Alin, S. R., … Zeng, J. (2025). Global Carbon Budget 2024. *Earth System Science Data*, *17*(3), 965–1039. https://doi.org/10.5194/essd-17-965-2025

Hoesly, R., Smith, S. J., Prime, N., Ahsan, H., Suchyta, H., O’Rourke, P., Crippa, M., Klimont, Z., Guizzardi, D., Behrendt, J., Feng, L., Harkins, C., McDonald, B., Mott, A., McDuffie, A., Nicholson, M., & Wang, S. (2024). *CEDS v_2024_07_08 Release Emission Data*. Zenodo. https://doi.org/10.5281/zenodo.12803197

Li, H., Ilyina, T., Loughran, T., Spring, A., & Pongratz, J. (2023). Reconstructions and predictions of the global carbon budget with an emission-driven Earth system model. *Earth System Dynamics*, *14*(1), 101–119. https://doi.org/10.5194/esd-14-101-2023

Smith, C., Cummins, D. P., Fredriksen, H.-B., Nicholls, Z., Meinshausen, M., Allen, M., Jenkins, S., Leach, N., Mathison, C., & Partanen, A.-I. (2024). fair-calibrate v1.4.1: calibration, constraining, and validation of the FaIR simple climate model for reliable future climate projections. *Geoscientific Model Development*, *17*(23), 8569–8592. https://doi.org/10.5194/gmd-17-8569-2024

Smith, C., Walsh, T., Gillett, N., Hall, B., Hauser, M., Krummel, P., Lamb, W., Lamboll, R., Lan, X., Muhle, J., Palmer, M., Ribes, A., Schumacher, D., Seneviratne, S., Trewin, B., von Schuckmann, K., & Forster, P. (2024). *ClimateIndicator/data: Indicators of Global Climate Change 2023 revision 2* . Zenodo. https://doi.org/10.5281/zenodo.11388387

van Marle, M. J. E., Kloster, S., Magi, B. I., Marlon, J. R., Daniau, A.-L., Field, R. D., Arneth, A., Forrest, M., Hantson, S., Kehrwald, N. M., Knorr, W., Lasslop, G., Li, F., Mangeon, S., Yue, C., Kaiser, J. W., & van der Werf, G. R. (2017). Historic global biomass burning emissions for CMIP6 (BB4CMIP) based on merging satellite observations with proxies and fire models (1750–2015). *Geoscientific Model Development*, *10*(9), 3329–3357. https://doi.org/10.5194/gmd-10-3329-2017